Heliyon

Interhemispheric disconnectivity in the sensorimotor network in bipolar disorder revealed by functional connectivity and diffusion tensor imaging analysis

Takuya Ishida [a,b,*]**, Tomohiro Donishi** [a]**, Jun Iwatani** [b]**, Shinichi Yamada** [b]**, Shun Takahashi** [b]**, Satoshi Ukai** [b]**, Kazuhiro Shinosaki** [b]**, Masaki Terada** [c]**, Yoshiki Kaneoke** [a]

[a] *Department of System Neurophysiology, Graduate School of Wakayama Medical University, 811-1 Kimiidera, Wakayama 641-8509, Japan*

[b] *Department of Neuropsychiatry, Graduate School of Wakayama Medical University, 811-1 Kimiidera, Wakayama 641-8509, Japan*

[c] *Wakayama-Minami Radiology Clinic, 870-2 Kimiidera, Wakayama 641-0012, Japan*

* Corresponding author at: Department of System Neurophysiology of Wakayama Medical University, 811–1 Kimiidera, Wakayama 641–8509, Japan.

E-mail address: ishitaku@wakayama-med.ac.jp (T. Ishida).

Abstract

Background: Little is known regarding interhemispheric functional connectivity (FC) abnormalities via the corpus callosum in subjects with bipolar disorder (BD), which might be a key pathophysiological basis of emotional processing alterations in BD.

Methods: We performed tract-based spatial statistics (TBSS) using diffusion tensor imaging (DTI) in 24 healthy control (HC) and 22 BD subjects. Next, we

analyzed the neural networks with independent component analysis (ICA) in 32HC and 25 BD subjects using resting-state functional magnetic resonance imaging.

Results: In TBSS analysis, we found reduced fractional anisotropy (FA) in the corpus callosum of BD subjects. In ICA, functional within-connectivity was reduced in two clusters in the sensorimotor network (SMN) (right and left primary somatosensory areas) of BD subjects compared with HCs. FC between the two clusters and FA values in the corpus callosum of BD subjects was significantly correlated. Further, the functional within-connectivity was related to Young Mania Rating Scale (YMRS) total scores in the right premotor area in the SMN of BD subjects.

Limitations: Almost all of our BD subjects were taking several medications which could be a confounding factor.

Conclusions: Our findings suggest that interhemispheric FC dysfunction in the SMN is associated with the impaired nerve fibers in the corpus callosum, which could be one of pathophysiological bases of emotion processing dysregulation in BD patients.

Keywords: Neuroscience, Medical imaging, Psychiatry

1. Introduction

Bipolar disorder (BD) is a chronic and severe disease with recurrent episodes of mania and depression, leading to decreased quality of life and increased burden on health care services (Hahn et al., 2014). Although many neurobiological alterations have been reported in BD (Frangou, 2014; Rey et al., 2016), its pathophysiological mechanism is still unknown (Bellani et al., 2016).

Magnetic resonance imaging (MRI) studies have revealed white matter (WM) microstructural abnormalities in the corpus callosum of BD subjects (Barnea-Goraly et al., 2009; Chaddock et al., 2009; Matsuoka et al., 2017; Sarrazin et al., 2014) and interhemispheric functional connectivity (FC) abnormalities in BD (Wang et al., 2015). This leads to a plausible hypothesis that interhemispheric functional disconnectivity via the corpus callosum has a key role in BD pathophysiology. However, little is known about the relationship of interhemispheric functional disconnectivity and structural alterations in the corpus callosum.

Yasuno and colleagues (Yasuno et al., 2016) investigated the relationship in patients with BD type II (BDII). Using a region-of-interest (ROI) FC approach, they selected 8 pairs of homotopic ROIs in the frontal regions and found a correlation between fractional anisotropy (FA) values in the corpus callosum and FC between homotopic regions of the ventral prefrontal cortex and insula. They found lower FC between these regions in BDII patients compared with major depressive disorder patients. However, no study has investigated the association

between interhemispheric FC and FA values in the corpus callosum, both of which have been shown to be lower in BD subjects than in healthy controls (HCs).

To address this issue, we examined tract-based spatial statistics (TBSS) using diffusion tensor imaging (DTI) to identify WM microstructural alterations in BD subjects compared with those in HCs and we employed independent component analysis (ICA) using resting-state functional MRI (rs-fMRI) to identify the regions whose within-connectivity in each resting-state network (RSN) was significantly different between HC and BD subjects. Since recent studies using rs-fMRI have revealed that several RSNs played an important pathophysiological role in BD, we adopted the following RSNs: the default mode network (DMN) (Meda et al., 2014), which is involved in self-relevant processing (Andrews-Hanna et al., 2010; Greicius et al., 2003); the left and right central executive network (CEN) (Lois et al., 2014; Najt et al., 2013), which is involved in information manipulation and decision-making behaviors (Uddin et al., 2011); the salience network (SN) (Teng et al., 2013), which is involved in switching the functions of other networks (Bonnelle et al., 2012; Seeley et al., 2007); and the sensorimotor network (SMN) (Martino et al., 2016), which is involved in sensory processing and motor tasks (Biswal et al., 1995; Huang et al., 2015). When we found a microstructural alteration in the corpus callosum with TBSS and symmetrical abnormal FC regions with ICA in BD subjects, we next calculated FC between these interhemispheric regions using a seed-based connectivity method and investigated whether the FA values in the corpus callosum were correlated with FC. It is worthwhile noting that we determine the interhemispheric regions whose FC was to be investigated with whole brain analysis using ICA to remove any preconceived hypotheses. We focused our investigation on those regions whose within-connectivity in each RSN for BD was significantly different from that for HC because we thought abnormal RSN component plays essentially important roles for pathological mechanism of BD. If we found abnormal within-connectivity in symmetrical regions in the same RSN, we hypothesized that those within-connectivity alterations were due to interhemispheric synchronization abnormalities via the abnormal transcallosal fibers (Andoh and Matsushita, 2015). As far as we know, this is the first study to examine the association between interhemispheric functional alterations and their underpinning of the structural abnormalities in BD subjects in direct comparison with HCs. FC between the two clusters of SMN and FA values in the corpus callosum of BD subjects was significantly correlated, while a negative correlation between the two parameters was found for HC subjects.

2. Methods

2.1. Participants

This study was carried out in accordance with the Declaration of Helsinki and was approved by the Ethics Committee of Wakayama Medical University. Written informed consent was obtained from all subjects.

Twelve subjects with BD type I (BDI; 8 males and 4 females) and 15 with BDII (9 males and 6 females) were recruited from outpatient departments at Wakayama Medical University Hospital and Wakayama Prefectural Mental Health Care Center. Diagnosis of BD was made according to the Diagnostic and Statistical Manual of Mental Disorders, Fourth Edition, by two independent psychiatrists who were certified by the Japanese Society for Psychiatry and Neurology. One had more than 10 years of clinical experience. Thirty-two age-matched HC volunteers (19 males and 13 females) were also recruited from these two institutions. All HC subjects were given a standard medical examination by two independent psychiatrists before they were recruited. They were deemed healthy and did not have any systemic or neurological illness, mental retardation, or head injury causing concussion. Table 1 shows the demographic data, including neuropsychological scales and clinical characteristics, of the subjects.

2.2. Clinical ratings

Experienced psychiatrists clinically rated the BD subjects prior to MRI acquisition. We assessed the severity of their symptoms using the Hamilton Rating Scale for Depression (HAMD) (Hamilton, 1967) and the Young Mania Rating Scale (YMRS) (Young et al., 1978). Premorbid intelligence quotient was estimated using the Japanese Adult Reading Test (JART) (Matsuoka et al., 2006) with 25 Japanese

Table 1. Demographic and clinical characteristics.

	HC	BD	Group difference *p*-value (test)
Age, years	37.8 ± 9.87	43.4 ± 13.6	0.0744 (*t*-test)[*]
Gender (M/F)	19/13	17/10	0.778 (χ^2test)[*]
JART	-	101 ± 10.4	-
YMRS	-	1.88 ± 2.80	-
HAMD	-	4.69 ± 5.74	-
Lithium, n	-	19	-
Anticonvulsant, n	-	11	-
Antidepressant, n	-	3	-
Antipsychotic, n	-	10	-

[*] Group difference between the HC and BD subjects.

ideographic script (Kanji) compound words, which is the Japanese version of the National Adult Reading Test (Nelson, 1982). One BD subject could not complete the YMRS and HAMD. All but one BD subjects took a range of medications, including lithium, anticonvulsants, and antipsychotics.

2.3. MRI acquisition

Scans were performed using 3.0 Tesla MRI (Philips, Amsterdam, the Netherlands) with a 32-channel head coil (SENSE Head 32CH) to obtain brain structural and resting state functional images from each subject. The mechanical sounds produced during the MRI procedure were minimized by the use of both earplugs and headphones. T1-weighted images were acquired using a 3D T1-weighted fast field echo sequence: TR, 7.0 ms; TE, 3.3 ms; FOV, 220 mm; matrix scan, 256; slice thickness, 0.9 mm; and flip angle, 10°.

DTI was performed with a single-shot spin-echo echo-planar imaging diffusion sequence in 15 directions. The DTI scan duration was 4 min 4 s with 935 images obtained. Other DTI parameters included: TR/TE, 6421/69 ms; FOV, 224 mm; flip angle, 90°; 55 slices; acquisition voxel size, $2.0 \times 2.0 \times 2.5$ mm; slice thickness, 2.5 mm; slice gap, 0 mm; and 2b-values, 0 and 1000. As 8HC and 5 BD subjects could not complete DTI acquisition, we acquired DTI for 24HC and 22 BD (11 BDI and 11 BDII) subjects.

The resting-state fMRI scan images were obtained using a gradient-echo echo-planar pulse sequence sensitive to BOLD contrast (Ogawa et al., 1990): TR, 3000 ms; TE, 30 ms; FOV, 192 mm; matrix scan, 64; slice thickness, 3 mm; and flip angle, 80°. Two runs, each with 105 volumes (for 5 min 15 s), were administered to each subject. Precautions were taken to minimize subjects' motion during the MRI study by instructing them to remain as still as possible with their eyes closed. We acquired fMRI data for 32HC and 27 BD (13 BDI and 14 BDII) subjects.

2.4. DTI data processing

DTI data were processed using programs in the FMRIB Software Library (FSL) version 5.0.5 (Smith et al., 2004) and TBSS (Smith et al., 2006). Source data were corrected for eddy currents and head motion by registering all data to the first b = 0 image with affine transformation. Each subject's head motion was assessed by means of translation/rotation, and all subjects in this study had less than 2 mm translation and 2° rotation. We also examined the group differences in translation and rotation of head movements according the following formula (Liu et al., 2008):

$$\text{Translation/Rotation} = \frac{1}{n-1}\sum_{i=2}^{n}\sqrt{|x_i - x_{i-1}|^2 + |y_i - y_{i-1}|^2 + |z_i - z_{i-1}|^2} \qquad (1)$$

where n is the number of points of the time series (here n = 16), and x_i, y_i, and z_i are translations/rotations at i-th time point in the x, y, and z directions, respectively.

The Brain Extraction Tool was used to create a binary mask from the non-diffusion weighted data (Smith, 2002), and the diffusion tensor and associated parameters such as FA were calculated using the DTIFIT program implemented in FSL. Non-linear transformation and affine registration were performed to normalize all FA data into a standard space using the nonlinear registration tool FNIRT. Normalized FA images were averaged to create a mean FA image, and a mean FA skeleton was created by taking the centers of all tracts common to all subjects. The voxel values of each subject's FA map were projected onto the skeleton by searching the local maxima along the perpendicular direction from the skeleton. A two-sample *t*-test was performed on skeletonized FA data with age as a nuisance covariate using permutation-based nonparametric inference (Nichols and Holmes, 2002). The number of permutations was set to 5000 and the result was corrected for multiple comparisons using the threshold-free cluster enhancement method. The threshold for significance was set at $p < 0.05$. Before comparing the HC and BD groups, we checked if there were any differences (at a significance level of $p < 0.05$ corrected for multiple comparisons with permutation test) between BDI and BDII subjects.

2.5. fMRI data preprocessing

fMRI data were analyzed using SPM8 (http://www.fil.ion.ucl.ac.uk/spm/) and in-house software with MATLAB (MathWorks, Natick, MA, USA). The initial 3 volumes were discarded to eliminate equilibration effects, leaving 102 consecutive volumes per session, and slice-timing correction was performed, followed by spatial realignment. Spatial normalization was achieved by 12-parameter affine transformation to the International Consortium for Brain Mapping Echo-Planar Imaging template in SPM8. Each image was resampled to 2 mm isotropic voxels and spatially smoothed with an 8-mm Gaussian kernel. Next, temporal band-pass filtering (0.01–0.1 Hz) was performed to reduce the effects of low-frequency drift and high-frequency noise (Lowe et al., 1998). Anatomical CompCor (Behzadi et al., 2007; Chai et al., 2012) was used to exclude the nonphysiological signals. Briefly, structural images were normalized and segmented into the cerebrospinal fluid (CSF), WM, and gray matter, which were generated using SPM8 with a probability threshold of 99%. The WM and CSF masks were eroded by one voxel to minimize partial voluming with gray matter and were used as noise ROIs. Signals from the WM and CSF ROIs were extracted from the unsmoothed functional volumes, and their 5 principal components were used as nuisance covariates of non-neural sources. Then, these 5 non-neural components and Friston's 24-parameter model (Friston et al., 1996) were removed from the data through linear regression. Scans with head motion exceeding 2 mm or 2° of maximum rotation through the run were discarded. Further, we examined the group

differences in translation and rotation of head movements based on formula (1) (Liu et al., 2008), in a similar way as for DTI preprocessing. Two BD type I subjects had to be removed from the analyses, resulting in a total of 32HC, 11 BDI, and 14 BDII subjects. Further we also examined the group differences in translation and rotation of head movements according the same formula (1) (Liu et al., 2008) used in DTI processing.

2.6. ICA

The group ICA tool of the fMRI toolbox (GIFT; version 3.0a; http://icatb. sourceforge.net) was used to perform group spatial ICA. Using the minimum description length criteria, we analyzed a mean of 19 components for each subject. An initial data reduction step was performed using principal components analysis and was followed by an independent component estimation that produced spatial maps and time courses with FAST ICA (Meda et al., 2012). Group ICA was calculated by back reconstruction including dual regression for each participant. The offset was calculated using the mean component maps that were subtracted from the subject component maps. The mean ICA components were transformed to z-scores with the time course of the relevant component. We performed group ICA without differentiating between the HC and BD subjects to ensure that the same components were identified in each group. We identified 6 ICs as RSNs of interest as follows. First, we carried out the spatial template matching procedure using the template of the DMN provided in the GIFT toolbox, and components that matched with the templates were selected as DMNs. The other four components of the RSN were identified with visual inspection as follows. The right and left CEN include the dorsolateral prefrontal cortex and posterior cingulate cortex as key regions (Uddin et al., 2011). The SN includes the dorsal anterior cingulate cortex and insular cortex (Bonnelle et al., 2012; Seeley et al., 2007). The SMN includes the somatosensory and motor cortices (Biswal et al., 1995; Huang et al., 2015). The averaged ICA component z-score map of the two sessions for each subject was calculated to perform statistical analyses. One-sample t-tests were carried out to determine anatomical regions within each network at a threshold of $p < 0.05$ FWE corrected. To identify the significantly different regions between HC and BD subjects within each RSN, two-sample t-tests were performed for each RSN masked by the regions identified in one-sample t-tests with age as a nuisance covariate. The statistically significant threshold was set at $p < 0.001$ uncorrected for height and a cluster $p < 0.05$ uncorrected for extension. Before comparing the HC and BD groups, we checked if there were any differences (at a significance level of $p < 0.05$ corrected for multiple comparisons with cluster-wise FWE) between BDI and BDII subjects.

2.7. Correlation between corpus callosum FA values and FC across the interhemispheric pairs of regions

We found that the FA values of BD patients were significantly reduced in the corpus callosum in TBSS and that within-network connectivity in the sensorimotor network was lower in two clusters, each of which belonged to each hemisphere symmetrically, for BD subjects compared with HCs in ICA analyses. Thus, we conducted seed-based FC analysis to compute interhemispheric FC between the two clusters found in ICA analysis and investigated the association between this FC and microstructural abnormalities in the corpus callosum. We extracted the mean time course of each cluster and calculated correlation coefficients between them. Further, we transformed these correlation coefficients to z scores with sample size adjustment using autocorrelation of the mean time-series from each ROI (Kaneoke et al., 2012; Ueyama et al., 2013) for each subject. The averaged z score of the two sessions in each subject was calculated to perform statistical analyses. We extracted the mean FA values in the identified region with TBSS analysis within the corpus callosum using the JHU DTI-based WM Atlas (http://cmrm.med.jhmi.edu) (Mori et al., 2008). Further, we calculated the mean FA values in the identified regions with TBSS within the corpus callosum where the primary sensory nerve fibers dominantly pass based on the Hofer and Frahm's method (Hofer and Frahm, 2006). Briefly, we defined the corpus callosum region where most of the fibers for the primary sensorimotor areas pass as the posterior one-third minus posterior one-fourth regions (MNI y coordinate is in the range [-23, −17]), which was defined as 'region IV' in Hofer and Frahm's study (Hofer and Frahm, 2006). Then, we performed partial correlation analysis between these FCs and the mean FA values in the corpus callosum region (both the whole corpus callosum regions and region IV) found in TBSS with age as a nuisance covariate.

2.8. Multiple regression analysis for ICA in SMN

We performed multiple regression analyses to investigate the relationships among the within-network connectivity (limited to aberrant network: SMN), age, JART, YMRS, and HAMD. Age, JART, YMRS, and HAMD were included as covariates. The statistical threshold was set at $p < 0.001$ uncorrected for height and a cluster $p < 0.05$ uncorrected for extension.

3. Results

3.1. Demographic and clinical data

Table 1 shows the demographic and clinical data of the subjects. None of the scores differed significantly between the two groups. Further, the demographic data of the subjects included in the analyses of fMRI and DTI are shown in Table 2.

Table 2. Demographic and clinical characteristics of the subjects included in DTI and fMRI analyses.

		HC	BD	Group difference *p*-value (test)
DTI	Age, years	36.0 ± 9.48	41.9 ± 13.3	0.0875 (*t*-test)[*]
	Gender (M/F)	12/12	13/9	0.536 (χ^2test)[*]
	JART	-	101 ± 11.0	-
	YMRS	-	1.86 ± 2.95	-
	HAMD	-	5.00 ± 6.13	-
fMRI	Age, years	37.8 ± 9.87	41.7 ± 12.6	0.194 (*t*-test)[*]
	Gender (M/F)	19/13	15/10	0.962 (χ^2 test)[*]
	JART	-	101 ± 10.6	-
	YMRS	-	1.96 ± 2.84	-
	HAMD	-	4.88 ± 5.78	-

[*] Group difference between the HC and BD subjects.

3.2. TBSS analysis

Head motion parameters for the HC and BD groups were checked with a *t*-test, which revealed no significant difference between the groups (Table 3).

We found no statistically different region between BDI and BDII subjects. Thus, BDI and BDII data were treated as one BD group for the subsequent analysis. FA values were significantly lower in the body of the corpus callosum and in the left corona radiata of the BD group compared to the HC group (Fig. 1).

3.3. ICA

Head motion parameters for the HC and BD groups were checked with a *t*-test, which revealed no significant difference between the groups (Table 3).

Table 3. Head motion parameters.

|		HC	BP	Group difference *p*-value(test)
DTI	translation (mm)	0.378 ± 0.150	0.334 ± 0.150	0.321 (*t*-test)
	rotation (rad)	0.0034 ± 0.0011	0.0031 ± 0.0010	0.280 (*t*-test)
fMRI (session1)	translation (mm)	0.0603 ± 0.0410	0.0534 ± 0.0480	0.562 (*t*-test)
	rotation (rad)	0.000778 ± 0.000305	0.000730 ± 0.000308	0.557 (*t*-test)
fMRI (session2)	translation (mm)	0.0392 ± 0.0178	0.0371 ± 0.0185	0.661 (*t*-test)
	rotation (rad)	0.000665 ± 0.000242	0.000675 ± 0.000535	0.924 (*t*-test)
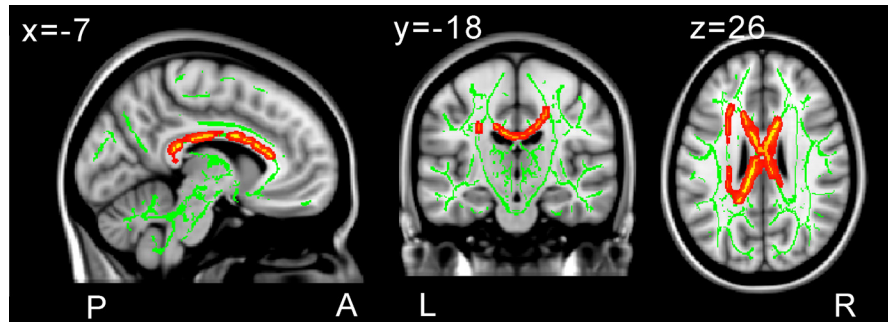
Fig. 1. Regions where the FA values were significantly different between the HC and BD subjects by TBSS analysis ($p < 0.05$, corrected for multiple comparisons by the permutation method with age as a nuisance covariate). The FA value was significantly reduced in the corpus callosum and in the left corona radiata of BD subjects compared with HCs.

We found two components corresponding to the anterior and posterior DMNs, respectively, based on the highest ranked correlation values (anterior DMN: 0.595, posterior DMN: 0.180). The other four components corresponding to the right and left CENs, SN, and SMN were identified as networks of interest (Fig. 2).

We found no statistically different region between BDI and BDII subjects in any RSN. Thus, BDI and BDII data were treated as one BD group for the subsequent analysis. For each identified component, a two-sample *t*-test was performed, and significantly reduced within-network connectivity was found in the primary somatosensory area in the SMN of the BD group (Fig. 3, Table 4). Two clusters were identified and each of them belonged to each hemisphere symmetrically. There were no significantly different regions for the other 5 ICA components.
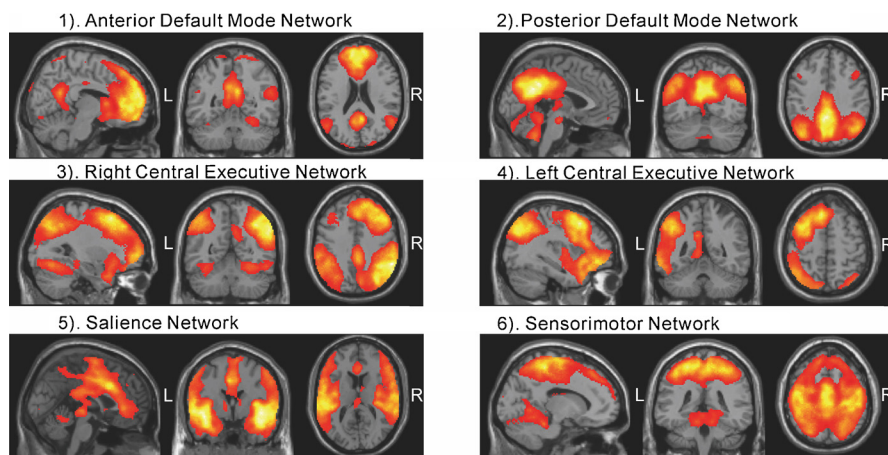

Fig. 2. Average six independent components for all HC and BD subjects. One-sample *t*-tests were carried out to determine anatomical regions within each network at a threshold of $p < 0.05$ FWE corrected.
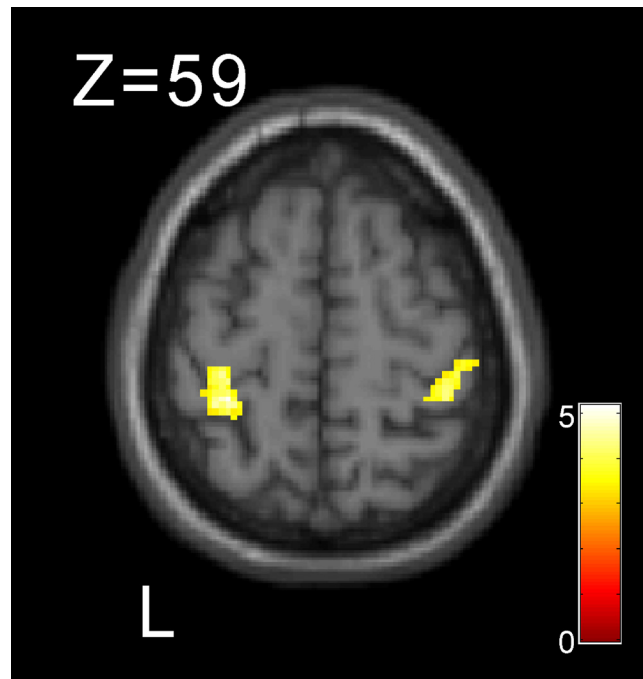
Fig. 3. The region where the within-connectivity was significantly different between HC and BD subjects in the sensorimotor network (SMN) by ICA using resting-state fMRI. Within-connectivity was significantly lower in two clusters in the somatosensory area for BD subjects compared with HCs, each of which was in the right and left somatosensory area, respectively. The statistical threshold was voxel-level $p < 0.001$ uncorrected for height and cluster-level $p < 0.05$ corrected for multiple comparisons.

3.4. Correlation between the mean FA values in the corpus callosum and FC between the two clusters in the SMN

FC between the two clusters found in the within-connectivity analysis in the SMN was positively correlated with the mean FA values both in the corpus callosum regions and in the region IV identified in TBSS with age as a nuisance covariate for the BD patients, while a negative correlation between those two parameters was found for the HC subjects (negative correlation for region IV was in trend-level). (Fig. 4).

Table 4. Regions with significantly different within-connectivity between the HC and BD subjects in the SMN by ICA using resting-state fMRI.

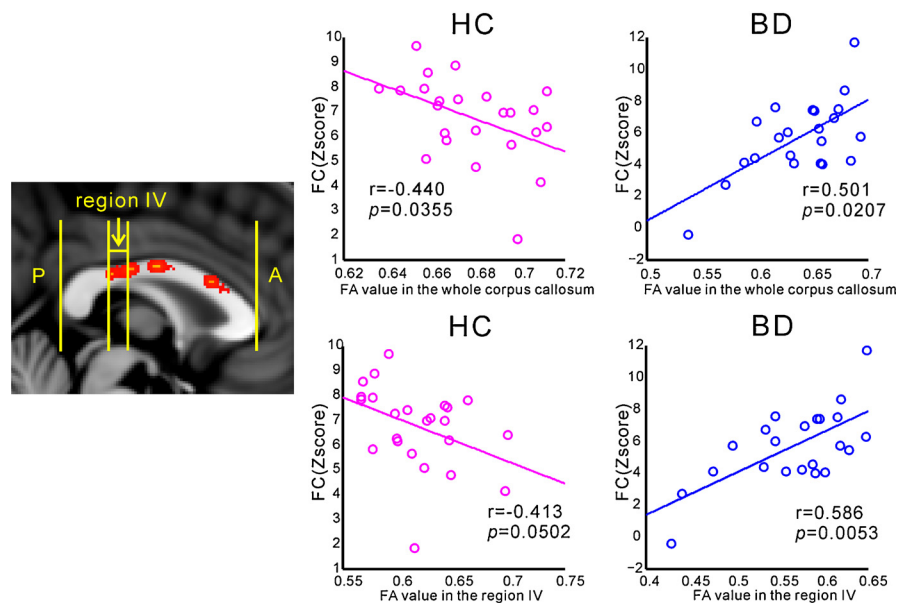| Identified regions	MNI (mm)			Z score	Number of voxels
	x	y	z		
Left somatosensory area	-28	-38	58	4.63	159
Right somatosensory area	36	-36	68	4.13	159

Fig. 4. The left brain sagittal slice (MNI coordinate: x=0) shows the regions where FA value was significantly lower for BD than for HC in both the whole and the region IV (where the fibers related to the primary sensorimotor areas exit, see text) in the corpus callosum. The right top two graphs show the association between the mean FA values in the identified region within the whole corpus callosum and the functional connectivity (FC) of the two identified somatosensory regions for HC and BD respectively. The right bottom two graphs show the association between the mean FA values in the region IV and the FC of the two somatosensory regions. A positive correlation between the two parameters was found in the BD subjects, while a negative correlation was observed in the HCs.

3.5. Multiple regression analysis for ICA in SMN

In the SMN, within-connectivity was positively correlated with the YMRS score in the right premotor region (Fig. 5, Table 5). In the right part of Fig. 5, the perpendicular axis shows the mean within-connectivity in the identified cluster and the horizontal axis shows the YMRS scores (r = 0.816, $p < 0.0005$). If one outlier whose YMRS score is high is removed from the analysis, the association between the mean within-connectivity in the identified cluster and the YMRS score is still significant (r = 0.511, $p = 0.0106$). No significant correlation was observed for the other clinical parameters (age, JART, and HAMD) in the SMN.

4. Discussion

Our main findings are as follows: 1) FA values were lower in the corpus callosum of the BD subjects compared with HCs with TBSS using DTI; 2) functional within-connectivity was reduced in two clusters, each of which was in the right and left somatosensory area, respectively, in the SMN of the BD subjects compared with HCs with ICA analysis using the resting fMRI method; 3) FC between the two clusters in the SMN and FA values in the significantly different regions in the
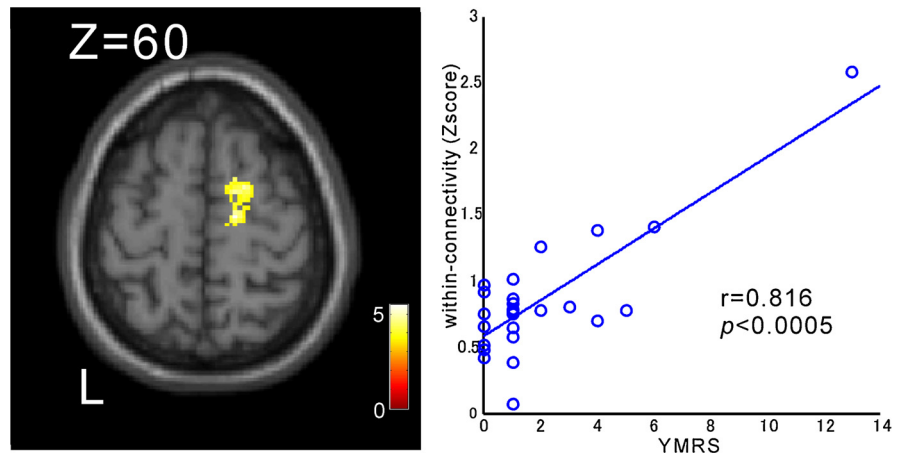
Fig. 5. Brain region in the SMN that was positively correlated with the total scores of YMRS in the BD subjects by multiple regression analysis. The graph shows the association between the YMRS scores and mean within-connectivity in the identified region. The statistical threshold was voxel-level $p <$ 0.001 uncorrected for height and cluster-level $p < 0.05$ corrected for multiple comparisons.

corpus callosum of the BD subjects was significantly correlated; and 4) functional within-connectivity was positively correlated with YMRS total scores in the right premotor area in the SMN of the BD subjects. To the best of our knowledge, this is the first study to show an association between interhemispheric FC of regions identified with different within-connectivity and an FA reduction in the corpus callosum of BD subjects.

Our ICA analysis manifested a within-connectivity reduction in the BD subjects compared with the HCs in somatosensory areas in the SMN. Somatosensory-related cortices are associated with representing intensions and actions in response to emotional stimuli such as facial expressions (Adolphs, 2003; Adolphs et al., 2000), and impairments in emotional processing are thought to be one of the most fundamental pathophysiological underpinnings of BD (Chen et al., 2011; Strakowski et al., 2012). Psychomotor symptoms, whose roles are related to SMNs, are considered to have a central clinical role in BD (Angst et al., 2013; Cassano et al., 2012). Kahdka and colleagues (Khadka et al., 2013) reported that BD patients with psychosis episodes showed increased FC in the superior frontal

Table 5. Brain region in the SMN that was positively correlated with the total scores of YMRS in the BD subjects by multiple regression analysis.

Identified region	MNI (mm)			Z score	Number of voxels
	x	**y**	**z**		
Right premotor area	16	-12	60	4.24	140

gyrus and medial frontal gyrus in the SMN compared with HCs. However, the abnormal pattern of FC reported by Kahdka et al. (Khadka et al., 2013) was opposite to our result, which may be due to the difference between the studied population samples. The BD subjects in the study of Kahdka et al. (Khadka et al., 2013) consisted of BDI patients with psychosis, while ours were comprised of both BDI and BDII patients. In addition, not all of the patients in our study had psychosis episodes. Seven out of 11 BDI patients and 1 out of 14 BDII patients had psychosis episodes.

Within-connectivity in the right premotor region in the SMN was positively correlated with the total score of YMRS for BD subjects (Fig. 5). In the study of Martino et al. (Martino et al., 2016), the slow (0.01–0.027 Hz) fractional SD DMN/ SMN balance was tilted toward the SMN in mania and was correlated with the total score of YMRS, which is consistent with our result. However, in our study, the correlation between the within-connectivity of the SMN and the YMRS score was found regardless of the phase in BD and no significant difference of within-connectivity in the DMN was identified between the two groups. This result strengthens the validity of the importance of the SMN in the pathological mechanism.

An abnormal FA value reduction in the corpus callosum of BD subjects was revealed in our TBSS analysis, which was supported by many previous studies (Barnea-Goraly et al., 2009; Chaddock et al., 2009; Macritchie et al., 2010; Marlinge et al., 2014; Yamada et al., 2015). In addition, the significant correlation between the FC of the two interhemispheric clusters whose within-connectivity was lower in the SMN of BD subjects and reduced FA values in the corpus callosum of BD subjects was found in our study (Fig. 4). A strong association between structural impairment in the corpus callosum and interhemispheric FC have been reported previously (Hinkley et al., 2012; Johnston et al., 2008; van der Knaap and van der Ham, 2011). Further, interhemispheric resting state FC abnormalities have also been found in BD subjects (Wang et al., 2015; Yasuno et al., 2016). Specifically, Yasuno et al. (Yasuno et al., 2016) found that FC between homotopic regions of the ventral prefrontal cortex and insula of BD subjects was positively correlated with FA values in the corpus callosum and they were significantly reduced compared with major depressive disorder patients. These observations are in line with our findings. Shobe (Shobe, 2014) suggested an interhemispheric interaction model via the corpus callosum that regulates emotion processing. Taken together with Adolphs' model (Adolphs, 2003; Adolphs et al., 2000), alterations of functional interhemispheric interactions via the corpus callosum in our findings result in the emotional dysregulation observed in subjects with BD. This direct correlation acquired by two entirely different MRI modalities supports our hypothesis that the association between interhemispheric functional

alterations and structural microabnormalities in the corpus callosum is one of the main pathophysiological factors in BD.

Interestingly, negative correlation between the corpus callosum FA and interhemispheric sensory FC was observed for the HCs. Previous studies reported that WM integrity in corpus callosum *motor* fibers was positively correlated with the strength of interhemispheric inhibition (Fling et al., 2013; Wahl et al., 2007), which helps to prevent interference of control processes between the two hemispheres (Fling et al., 2011; Muller-Oehring et al., 2007), and that increased resting state interhemispheric motor FC reflects the loss of the strength of interhemispheric inhibition (Fling et al., 2011; Langan et al., 2010). Accordingly, the negative correlation between interhemispheric FC in the somatosensory area and the FA value in the corpus callosum for HCs in our study might indicate increased interhemispheric inhibition in somatosensory function according to somatosensory fiber integrity in the corpus callosum, which is consistent with previous studies (Fling et al., 2013; Wahl et al., 2007). Thus, the positive relationship between the two parameters for BD group suggests that the interhemispheric inhibition in normal brain functional state is impaired in BD subjects. Collin et al. (Collin et al., 2016) reported that structural interhemispheric connectivity reduction in BD lead to deficit of global efficiency and to intellectual impairment for BD. Some mechanism for compensating the information transfer deficit between hemispheres via the corpus callosum abnormality might reduce the interhemispheric inhibition so that both hemispheres could be easily interacted with each other, and this loss of interhemispheric inhibition in BD subjects might lead to the emotional dysregulation and to the high impulsivity in BD subjects.

There are some limitations of the present study that need to be addressed. First, almost all BD patients were euthymic or depressed state (total scores of YMRS were less than 8 except for one patient). So we could not determine whether our result could be applied to the manic state. Second, almost all of our BD subjects were taking several medications, which might have some influence on resting state BOLD signals or brain structures. However, we did not find any relationship between the amount of medication (CPZ equivalent dose, the amount of sodium valproate or lithium) and our findings. Third, we might overlook the interhemispheric FC abnormalities in symmetrical regions which belong to other RSN than SMN. However, we focused our investigation on those regions whose within-connectivity in each RSN for BD was significantly different from that for HC because we thought abnormal RSN component was essentially important regions for pathological mechanism of BD.

In conclusion, we found a significant relationship in BD subjects between the FC of interhemispheric regions in SMN whose within-connectivity was lower in BD subjects than in HCs and reduced FA values in the corpus callosum. Further,

within-connectivity in the SMN of BD subjects was positively correlated with the total scores of YMRS in the right premotor region. These findings suggest that interhemispheric FC in the SMN via the corpus callosum is related to the dysregulation of emotion processing in BD patients, which is one of the main pathophysiological factors in BD.

Declarations

Author contribution statement

Takuya Ishida: Conceived and designed the experiments; Analyzed and interpreted the data; Contributed reagents, materials, analysis tools or data; Wrote the paper.

Tomohiro Donishi: Analyzed and interpreted the data; Contributed reagents, materials, analysis tools or data.

Jun Iwatani, Shinichi Yamada, Shun Takahashi, Satoshi Ukai, Kazuhiro Shinosaki, Masaki Terada: Performed the experiments.

Yoshiki Kaneoke: Conceived and designed the experiments; Wrote the paper.

Funding statement

Competing interest statement

The authors declare no conflict of interest.

Additional information

No additional information is available for this paper.

Acknowledgements

References

Adolphs, R., 2003. Cognitive neuroscience of human social behaviour. Nat. Rev. Neurosci. 4, 165–178.

Adolphs, R., Damasio, H., Tranel, D., Cooper, G., Damasio, A.R., 2000. A role for somatosensory cortices in the visual recognition of emotion as revealed by three-dimensional lesion mapping. J. Neurosci. 20, 2683–2690.

Andoh, J., Matsushita, R., 2015. Asymmetric Interhemispheric Transfer in the Auditory Network: Evidence from TMS, Resting-State fMRI, and Diffusion Imaging. J. Neurosci. 35, 14602–14611.

Andrews-Hanna, J.R., Reidler, J.S., Sepulcre, J., Poulin, R., Buckner, R.L., 2010. Functional-anatomic fractionation of the brain's default network. Neuron 65, 550–562.

Angst, J., Gamma, A., Bowden, C.L., Azorin, J.M., Perugi, G., Vieta, E., Young, A.H., 2013. Evidence-based definitions of bipolar-I and bipolar-II disorders among 5,635 patients with major depressive episodes in the Bridge Study: validity and comorbidity. Eur. Arch. Psychiatry Clin. Neurosci. 263, 663–673.

Barnea-Goraly, N., Chang, K.D., Karchemskiy, A., Howe, M.E., Reiss, A.L., 2009. Limbic and corpus callosum aberrations in adolescents with bipolar disorder: a tract-based spatial statistics analysis. Biol. Psychiatry 66, 238–244.

Behzadi, Y., Restom, K., Liau, J., Liu, T.T., 2007. A component based noise correction method (CompCor) for BOLD and perfusion based fMRI. NeuroImage 37, 90–101.

Bellani, M., Boschello, F., Delvecchio, G., Dusi, N., Altamura, C.A., Ruggeri, M., Brambilla, P., 2016. DTI and Myelin Plasticity in Bipolar Disorder: Integrating Neuroimaging and Neuropathological Findings. Front. Psychiatry 7, 21.

Biswal, B., Yetkin, F.Z., Haughton, V.M., Hyde, J.S., 1995. Functional connectivity in the motor cortex of resting human brain using echo-planar MRI. Magn. Reson. Med. 34, 537–541.

Bonnelle, V., Ham, T.E., Leech, R., Kinnunen, K.M., Mehta, M.A., Greenwood, R.J., Sharp, D.J., 2012. Salience network integrity predicts default mode network function after traumatic brain injury. Proc. Natl. Acad. Sci. USA 109, 4690–4695.

Cassano, G.B., Rucci, P., Benvenuti, A., Miniati, M., Calugi, S., Maggi, L., Pini, S., Kupfer, D.J., Maj, M., Fagiolini, A., Frank, E., 2012. The role of psychomotor activation in discriminating unipolar from bipolar disorders: a classification-tree analysis. J. Clin. Psychiatry 73, 22–28.

Chaddock, C.A., Barker, G.J., Marshall, N., Schulze, K., Hall, M.H., Fern, A., Walshe, M., Bramon, E., Chitnis, X.A., Murray, R., McDonald, C., 2009. White matter microstructural impairments and genetic liability to familial bipolar I disorder. Br. J. Psychiatry 194, 527–534.

Chai, X.J., Castanon, A.N., Ongur, D., Whitfield-Gabrieli, S., 2012. Anticorrelations in resting state networks without global signal regression. NeuroImage 59, 1420–1428.

Chen, C.H., Suckling, J., Lennox, B.R., Ooi, C., Bullmore, E.T., 2011. A quantitative meta-analysis of fMRI studies in bipolar disorder. Bipolar Disord. 13, 1–15.

Collin, G., van den Heuvel, M.P., Abramovic, L., Vreeker, A., de Reus, M.A., van Haren, N.E., Boks, M.P., Ophoff, R.A., Kahn, R.S., 2016. Brain network analysis reveals affected connectome structure in bipolar I disorder. Hum. Brain Mapp. 37, 122–134.

Fling, B.W., Benson, B.L., Seidler, R.D., 2013. Transcallosal sensorimotor fiber tract structure-function relationships. Hum. Brain Mapp. 34, 384–395.

Fling, B.W., Peltier, S.J., Bo, J., Welsh, R.C., Seidler, R.D., 2011. Age differences in interhemispheric interactions: callosal structure, physiological function, and behavior. Front. Neurosci. 5, 38.

Frangou, S., 2014. A systems neuroscience perspective of schizophrenia and bipolar disorder. Schizophr. Bull. 40, 523–531.

Friston, K.J., Williams, S., Howard, R., Frackowiak, R.S., Turner, R., 1996. Movement-related effects in fMRI time-series. Magn. Reson. Med. 35, 346–355.

Greicius, M.D., Krasnow, B., Reiss, A.L., Menon, V., 2003. Functional connectivity in the resting brain: a network analysis of the default mode hypothesis. Proc. Natl. Acad. Sci. USA 100, 253–258.

Hahn, C., Lim, H.K., Lee, C.U., 2014. Neuroimaging findings in late-onset schizophrenia and bipolar disorder. J. Geriatr. Psychiatry Neurol. 27, 56–62.

Hamilton, M., 1967. Development of a rating scale for primary depressive illness. Br. J. Soc. Clin. Psychol. 6, 278–296.

Hinkley, L.B., Marco, E.J., Findlay, A.M., Honma, S., Jeremy, R.J., Strominger, Z., Bukshpun, P., Wakahiro, M., Brown, W.S., Paul, L.K., Barkovich, A.J., Mukherjee, P., Nagarajan, S.S., Sherr, E.H., 2012. The role of corpus callosum development in functional connectivity and cognitive processing. PloS One 7, e39804.

Hofer, S., Frahm, J., 2006. Topography of the human corpus callosum revisited––comprehensive fiber tractography using diffusion tensor magnetic resonance imaging. NeuroImage 32, 989–994.

Huang, S., Li, Y., Zhang, W., Zhang, B., Liu, X., 2015. Multisensory Competition Is Modulated by Sensory Pathway Interactions with Fronto-Sensorimotor and Default-Mode Network Regions. J. Neurosci. 35, 9064–9077.

Johnston, J.M., Vaishnavi, S.N., Smyth, M.D., Zhang, D., He, B.J., Zempel, J.M., Shimony, J.S., Snyder, A.Z., Raichle, M.E., 2008. Loss of resting interhemispheric functional connectivity after complete section of the corpus callosum. J. Neurosci. 28, 6453–6458.

Kaneoke, Y., Donishi, T., Iwatani, J., Ukai, S., Shinosaki, K., Terada, M., 2012. Variance and autocorrelation of the spontaneous slow brain activity. PloS One 7, e38131.

Khadka, S., Meda, S.A., Stevens, M.C., Glahn, D.C., Calhoun, V.D., Sweeney, J. A., Tamminga, C.A., Keshavan, M.S., O'Neil, K., Schretlen, D., Pearlson, G.D., 2013. Is aberrant functional connectivity a psychosis endophenotype: A resting state functional magnetic resonance imaging study. Biol. Psychiatry 74, 458–466.

Langan, J., Peltier, S.J., Bo, J., Fling, B.W., Welsh, R.C., Seidler, R.D., 2010. Functional implications of age differences in motor system connectivity. Front. Syst. Neurosci. 4, 17.

Liu, Y., Liang, M., Zhou, Y., He, Y., Hao, Y., Song, M., Yu, C., Liu, H., Liu, Z., Jiang, T., 2008. Disrupted small-world networks in schizophrenia. Brain 131, 945–961.

Lois, G., Linke, J., Wessa, M., 2014. Altered functional connectivity between emotional and cognitive resting state networks in euthymic bipolar I disorder patients. PloS One 9, e107829.

Lowe, M.J., Mock, B.J., Sorenson, J.A., 1998. Functional connectivity in single and multislice echoplanar imaging using resting-state fluctuations. NeuroImage 7, 119–132.

Macritchie, K.A., Lloyd, A.J., Bastin, M.E., Vasudev, K., Gallagher, P., Eyre, R., Marshall, I., Wardlaw, J.M., Ferrier, I.N., Moore, P.B., Young, A.H., 2010. White matter microstructural abnormalities in euthymic bipolar disorder. Br. J. Psychiatry 196, 52–58.

Marlinge, E., Bellivier, F., Houenou, J., 2014. White matter alterations in bipolar disorder: potential for drug discovery and development. Bipolar Disord. 16, 97–112.

Martino, M., Magioncalda, P., Huang, Z., Conio, B., Piaggio, N., Duncan, N.W., Rocchi, G., Escelsior, A., Marozzi, V., Wolff, A., Inglese, M., Amore, M., Northoff, G., 2016. Contrasting variability patterns in the default mode and

sensorimotor networks balance in bipolar depression and mania. Proc. Natl. Acad. Sci. USA 113, 4824–4829.

Matsuoka, K., Uno, M., Kasai, K., Koyama, K., Kim, Y., 2006. Estimation of premorbid IQ in individuals with Alzheimer's disease using Japanese ideographic script (Kanji) compound words: Japanese version of National Adult Reading Test. Psychiatry Clin. Neurosci. 60, 332–339.

Matsuoka, K., Yasuno, F., Kishimoto, T., Yamamoto, A., Kiuchi, K., Kosaka, J., Nagatsuka, K., Iida, H., Kudo, T., 2017. Microstructural Differences in the Corpus Callosum in Patients With Bipolar Disorder and Major Depressive Disorder. J. Clin. Psychiatry 78, 99–104.

Meda, S.A., Gill, A., Stevens, M.C., Lorenzoni, R.P., Glahn, D.C., Calhoun, V.D., Sweeney, J.A., Tamminga, C.A., Keshavan, M.S., Thaker, G., Pearlson, G.D., 2012. Differences in resting-state functional magnetic resonance imaging functional network connectivity between schizophrenia and psychotic bipolar probands and their unaffected first-degree relatives. Biol. Psychiatry 71, 881–889.

Meda, S.A., Ruano, G., Windemuth, A., O'Neil, K., Berwise, C., Dunn, S.M., Boccaccio, L.E., Narayanan, B., Kocherla, M., Sprooten, E., Keshavan, M.S., Tamminga, C.A., Sweeney, J.A., Clementz, B.A., Calhoun, V.D., Pearlson, G.D., 2014. Multivariate analysis reveals genetic associations of the resting default mode network in psychotic bipolar disorder and schizophrenia. Proc. Natl. Acad. Sci. USA 111, E2066–2075.

Mori, S., Oishi, K., Jiang, H., Jiang, L., Li, X., Akhter, K., Hua, K., Faria, A.V., Mahmood, A., Woods, R., Toga, A.W., Pike, G.B., Neto, P.R., Evans, A., Zhang, J., Huang, H., Miller, M.I., van Zijl, P., Mazziotta, J., 2008. Stereotaxic white matter atlas based on diffusion tensor imaging in an ICBM template. NeuroImage 40, 570–582.

Muller-Oehring, E.M., Schulte, T., Raassi, C., Pfefferbaum, A., Sullivan, E.V., 2007. Local-global interference is modulated by age, sex and anterior corpus callosum size. Brain Res. 1142, 189–205.

Najt, P., Bayer, U., Hausmann, M., 2013. Right fronto-parietal dysfunction underlying spatial attention in bipolar disorder. Psychiatry Res. 210, 479–484.

Nelson, H.E., 1982. National Adult Reading Test (NART): Test Manual. NFER-Nelson, Windsor (UK).

Nichols, T.E., Holmes, A.P., 2002. Nonparametric permutation tests for functional neuroimaging: a primer with examples. Hum. Brain Mapp. 15, 1–25.

Ogawa, S., Lee, T.M., Kay, A.R., Tank, D.W., 1990. Brain magnetic resonance imaging with contrast dependent on blood oxygenation. Proc. Natl. Acad. Sci. USA 87, 9868–9872.

Rey, G., Piguet, C., Benders, A., Favre, S., Eickhoff, S.B., Aubry, J.M., Vuilleumier, P., 2016. Resting-state functional connectivity of emotion regulation networks in euthymic and non-euthymic bipolar disorder patients. Eur. Psychiatry 34, 56–63.

Sarrazin, S., Poupon, C., Linke, J., Wessa, M., Phillips, M., Delavest, M., Versace, A., Almeida, J., Guevara, P., Duclap, D., Duchesnay, E., Mangin, J.F., Le Dudal, K., Daban, C., Hamdani, N., D'Albis, M.A., Leboyer, M., Houenou, J., 2014. A multicenter tractography study of deep white matter tracts in bipolar I disorder: psychotic features and interhemispheric disconnectivity. JAMA Psychiatry 71, 388–396.

Seeley, W.W., Menon, V., Schatzberg, A.F., Keller, J., Glover, G.H., Kenna, H., Reiss, A.L., Greicius, M.D., 2007. Dissociable intrinsic connectivity networks for salience processing and executive control. J. Neurosci. 27, 2349–2356.

Shobe, E.R., 2014. Independent and collaborative contributions of the cerebral hemispheres to emotional processing. Front. Hum. Neurosci. 8, 230.

Smith, S.M., 2002. Fast robust automated brain extraction. Hum. Brain Mapp. 17, 143–155.

Smith, S.M., Jenkinson, M., Johansen-Berg, H., Rueckert, D., Nichols, T.E., Mackay, C.E., Watkins, K.E., Ciccarelli, O., Cader, M.Z., Matthews, P.M., Behrens, T.E., 2006. Tract-based spatial statistics: voxelwise analysis of multi-subject diffusion data. NeuroImage 31, 1487–1505.

Smith, S.M., Jenkinson, M., Woolrich, M.W., Beckmann, C.F., Behrens, T.E., Johansen-Berg, H., Bannister, P.R., De Luca, M., Drobnjak, I., Flitney, D.E., Niazy, R.K., Saunders, J., Vickers, J., Zhang, Y., De Stefano, N., Brady, J.M., Matthews, P.M., 2004. Advances in functional and structural MR image analysis and implementation as FSL. NeuroImage 23 (Suppl 1), S208–219.

Strakowski, S.M., Adler, C.M., Almeida, J., Altshuler, L.L., Blumberg, H.P., Chang, K.D., DelBello, M.P., Frangou, S., McIntosh, A., Phillips, M.L., Sussman, J.E., Townsend, J.D., 2012. The functional neuroanatomy of bipolar disorder: a consensus model. Bipolar Disord. 14, 313–325.

Teng, S., Lu, C.F., Wang, P.S., Hung, C.I., Li, C.T., Tu, P.C., Su, T.P., Wu, Y.T., 2013. Classification of bipolar disorder using basal-ganglia-related functional connectivity in the resting state. Conference proceedings: Annual International Conference of the IEEE Engineering in Medicine and Biology Society. IEEE

Engineering in Medicine and Biology Society. Annual Conference 2013, 1057–1060.

Uddin, L.Q., Supekar, K.S., Ryali, S., Menon, V., 2011. Dynamic reconfiguration of structural and functional connectivity across core neurocognitive brain networks with development. J. Neurosci. 31, 18578–18589.

Ueyama, T., Donishi, T., Ukai, S., Ikeda, Y., Hotomi, M., Yamanaka, N., Shinosaki, K., Terada, M., Kaneoke, Y., 2013. Brain regions responsible for tinnitus distress and loudness: a resting-state FMRI study. PloS One 8, e67778.

van der Knaap, L.J., van der Ham, I.J., 2011. How does the corpus callosum mediate interhemispheric transfer? A review. Behav. Brain Res. 223, 211–221.

Wahl, M., Lauterbach-Soon, B., Hattingen, E., Jung, P., Singer, O., Volz, S., Klein, J.C., Steinmetz, H., Ziemann, U., 2007. Human motor corpus callosum: topography, somatotopy, and link between microstructure and function. J. Neurosci. 27, 12132–12138.

Wang, Y., Zhong, S., Jia, Y., Zhou, Z., Wang, B., Pan, J., Huang, L., 2015. Interhemispheric resting state functional connectivity abnormalities in unipolar depression and bipolar depression. Bipolar Disord. 17, 486–495.

Yamada, S., Takahashi, S., Ukai, S., Tsuji, T., Iwatani, J., Tsuda, K., Kita, A., Sakamoto, Y., Yamamoto, M., Terada, M., Shinosaki, K., 2015. Microstructural abnormalities in anterior callosal fibers and their relationship with cognitive function in major depressive disorder and bipolar disorder: a tract-specific analysis study. J. Affect. Disord. 174, 542–548.

Yasuno, F., Kudo, T., Matsuoka, K., Yamamoto, A., Takahashi, M., Nakagawara, J., Nagatsuka, K., Iida, H., Kishimoto, T., 2016. Interhemispheric functional disconnection because of abnormal corpus callosum integrity in bipolar disorder type II. BJPsych Open 2, 335–340.

Young, R.C., Biggs, J.T., Ziegler, V.E., Meyer, D.A., 1978. A rating scale for mania: reliability: validity and sensitivity. Br. J. Psychiatry 133, 429–435.